

## Remnant Polarization in Thin Films from a Columnar Liquid Crystal

Carel F. C. Fitié,<sup>†</sup> W. S. Christian Roelofs,<sup>‡</sup> Martijn Kemerink,<sup>\*,†</sup> and Rint P. Sijbesma<sup>\*,†</sup>

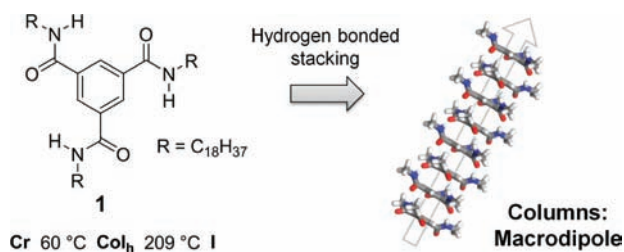
Laboratory of Macromolecular and Organic Chemistry and Department of Applied Physics, Eindhoven University of Technology, P.O. Box 513, 5600 MB, Eindhoven, The Netherlands

Received March 1, 2010; E-mail: m.kemerink@tue.nl; r.p.sijbesma@tue.nl

Organic thin films with a large remnant polarization are of great interest for diodes and nonvolatile memory devices.<sup>1</sup> Specifically, ferroelectric columnar liquid crystalline (LC) phases that feature stable, switchable polarization along the column axis have potential in ultrahigh density memory devices in which ultimately a single column can function as a memory element through manipulation of its macroscopic polarization.<sup>2a</sup> However, in spite of several research efforts, stable remnant polarization in such systems has not been observed.<sup>2</sup>

Here we show ferroelectric switching in a simple, hydrogen bonded LC phase. The polar order induced in the LC phase can be frozen by crystallization of the alkyl chains in the periphery of the columns yielding thin films with remnant polarization and an unprecedented high surface potential as shown by Scanning Kelvin Probe Microscopy (SKPM).

### Scheme 1



Previously, we have used discotic molecules with a benzene-1,3,5-tricarboxamide (BTA) core to design nanostructured materials.<sup>3</sup> BTAs are known to form supramolecular columnar assemblies with a helical structure through 3-fold hydrogen bonding between the amide groups connected to the core.<sup>4</sup> Irrespective of the helical sense of the columns, all amides point in the same direction and are stacked head-to-tail. Therefore, the individual dipole moments of the amides add up and result in a large, macroscopic dipole along the column axis (Scheme 1).<sup>5a</sup> Studies addressing the alignment of BTAs with an electric field in the LC state, the dielectric properties in organogels, and ferroelectric properties in the solid state prompted us to investigate the dielectric properties of LC thin films of BTAs.<sup>5</sup>

The BTA derivative with octadecyl side chains (**1**, Scheme 1) was introduced in glass LC cells with a spacing of 5  $\mu\text{m}$  that were coated with two transparent electrodes. At 150  $^{\circ}\text{C}$ , the hexagonal LC phase was aligned uniformly with the columns perpendicular to the electrodes by applying a DC field of 30  $\text{V}/\mu\text{m}$  as indicated by a black texture under observation by polarizing optical microscopy (POM). When the aligned sample was cooled down, a weakly birefringent texture was formed at  $\sim 60$   $^{\circ}\text{C}$  as a result of crystallization. Interestingly, the black texture reappeared when the sample was heated above the melting point of the crystalline phase without

a field across the cell suggesting that the basic columnar structure and its alignment are unaffected by the crystallization of the alkyl chains in the periphery. Wide angle X-ray scattering (WAXS) measurements after cooling from the LC phase confirmed that the hexagonal lattice and the columnar structure remain intact (see Supporting Information (SI)).

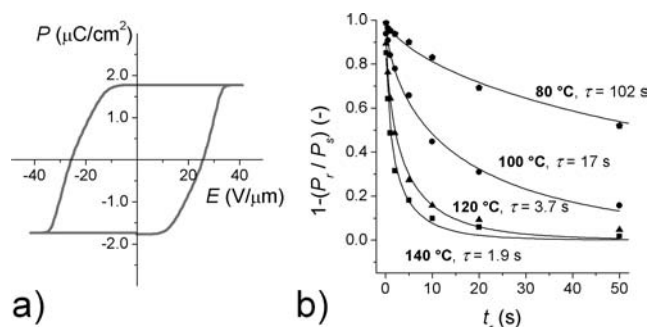


**Figure 1.** (a) Typical  $P$ - $E$  hysteresis loop for **1** (100  $^{\circ}\text{C}$ , 0.5 Hz). The polarization due to macrodipole inversion was estimated by integrating the peak that was observed in the cell response current after subtracting a baseline that takes both conductive and capacitive effects into account (see SI). (b) Normalized remaining polarization  $1 - (P_r/P_s)$  as a function of time ( $t_r$ ). The lines are stretched exponential fits to the data.

The current response induced by switching of the macrodipoles was measured under application of a triangular voltage wave over prealigned sample cells (0.1–5 Hz, 400  $\text{V}_{\text{p-p}}$ ). During these experiments the initial black POM texture remained unchanged indicating that the homeotropic alignment of the BTA columns is retained throughout the switching process. The polarization ( $P$ ) of the sample was evaluated as a function of the applied field ( $E$ ) by integrating the peak that was observed in the cell response current. The  $P$ - $E$  loops showed clear hysteresis as well as a concave and fairly symmetric shape indicative of ferroelectric behavior (Figure 1a). The spontaneous polarization ( $P_s$ ) and coercive field ( $E_c$ ) were determined from the axis crossings of the  $P$ - $E$  loops and resulted in values of 1.3–1.8  $\mu\text{C}/\text{cm}^2$  and 21–26  $\text{V}/\mu\text{m}$ , respectively.

The maximum switching frequency increased with temperature from 0.1 Hz at 70  $^{\circ}\text{C}$  to 5.0 Hz at 150  $^{\circ}\text{C}$ , while  $P_s$  remained fairly constant (see SI). The constant values for  $P_s$  indicate that the switching peak in the cell response originates from the reorientation of the macrodipoles and not from ionic or charge relaxation phenomena.<sup>2d,e</sup> Moreover, the effective dipole moment of the three amide bonds in **1** that was calculated based on the average  $P_s$ -value is 8.3 D (see SI). This value is in excellent agreement with the average dipole moments calculated for stacked BTAs in molecular modeling studies (9–14 D) and provides additional evidence for the origin of the switching behavior.<sup>5c,6</sup>

A separate set of experiments demonstrated that the spontaneous polarization in **1** has a finite lifetime in the LC state. After an initial poling pulse ( $E > E_c$ ), the field was removed for a period of time

<sup>†</sup> Laboratory of Macromolecular and Organic Chemistry.

<sup>‡</sup> Applied Physics.

( $t_r$ ) to allow the polarization to relax. Subsequently, a probe pulse was given with the same polarity and the current response of the cell was measured. If the spontaneous polarization is stable during  $t_r$ , the pulse will not change the polarization of the samples. Conversely, if the initial polarization is completely relaxed during  $t_r$ , the pulse will lead to a buildup of polarization and the integrated response signal ( $P_r$ ) will equal  $P_s$ . Figure 1b shows the normalized remaining polarization  $1 - (P_r/P_s)$  as a function of  $t_r$  at four different temperatures. The characteristic relaxation time ( $\tau$ ) of the polarization was estimated by fitting the data sets to a stretched exponential function (see SI). The  $\tau$ -values decreased with temperature from 102 to 1.9 s showing that the LC phase of **1** is not properly ferroelectric.

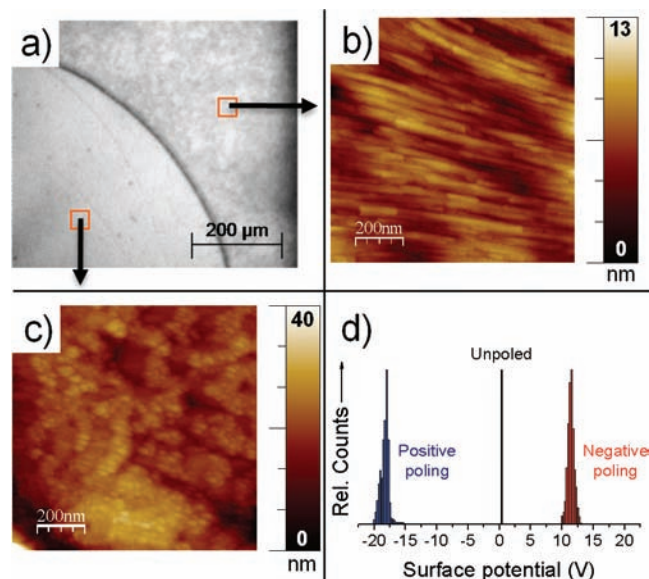


**Figure 2.** AFM and SKPM results for thin films of **1**. (a) Optical microscopy image showing the difference between aligned (bottom left) and unaligned (top right) sample areas. The red squares indicate the approximate positions at which the AFM images in b and c were made. (b) AFM height image of an unaligned thin film. (c) AFM height image of an aligned thin film. (d) Histogram of typical surface potentials observed by SKPM for positively poled, negatively poled, and unpoled thin films.

Interestingly, the crystallization of **1** freezes the polar order of the macrodipoles and can be employed to produce thin films with stable, remnant polarization. Thin films (300–400 nm) were spin-coated on glass plates coated with a transparent electrode. The films were locally aligned and poled using a liquid mercury electrode (140 °C,  $\sim 29$  V/ $\mu$ m). Then, the samples were cooled to room temperature while maintaining the field. The aligned and unaligned areas of the samples were clearly detectable by optical microscopy and had a completely different surface topography as observed by AFM (Figure 2a–c). In the unaligned areas the BTA columns lie parallel to the surface in bundles with a diameter of  $\sim 50$  nm. In the areas where the columns are aligned perpendicular to the surface, the AFM images show a top view of these bundles.

The surface potential of the thin films was measured by SKPM (typical data sets shown in Figure 2d). In unpoled samples, the surface potential was  $\sim 0$  V. When the samples were poled, we observed surface potentials with a polarity opposite to that of the mercury electrode used for poling. The absolute values of the surface potential were  $\pm 10$ – $20$  V for both positively and negatively poled samples. Such high values for the remaining surface potential

are unique, because the measured surface potential of ferroelectric materials is usually strongly reduced by screening effects due to mobile ionic and dipolar species in the system.<sup>7</sup> We believe that some screening also occurs in the BTA layers and that the experimental distribution in the absolute surface potentials is caused by small variations in the extent of screening. In line with the results of the lifetime measurements, the surface potential rapidly decreased to  $\sim 0$  V when the samples were heated above the melting point of the crystalline phase in the SKPM setup.

In conclusion, we have shown that the crystallization of the peripheral alkyl chains in a BTA derivative freezes the polar order of the macrodipoles present in the LC phase and can be used to obtain thin films with remnant polarization. This study highlights the potential of these materials to form nanostructured thin films that integrate remnant electric polarization with other functional properties for applications in organic diodes and asymmetric membranes. The switching mechanism in BTAs is currently explored in more detail by dielectric relaxation spectroscopy. Furthermore, we are investigating piezoelectric properties of the thin films and manipulation of the polarization on a local scale by SKPM.

**Acknowledgment.** The authors thank Prof. Dago de Leeuw and Dr. Kamal Asadi of the University of Groningen for stimulating discussions. Ben Norder and Dr. Eduardo Mendes of the Technical University of Delft are acknowledged for providing access to their WAXS setup. This work has been financially supported by The Netherlands Organization for Scientific Research, Chemical Sciences (NWO-CW).

**Supporting Information Available:** Experimental section, calorimetric data, WAXS data and indexing, full results switching experiments, typical cell response in lifetime measurements, additional SKPM and AFM data. This material is available free of charge via the Internet at <http://pubs.acs.org>.

## References

- (1) (a) Asadi, K.; de Leeuw, D. M.; de Boer, B.; Blom, P. W. M. *Nat. Mater.* **2008**, *7*, 547–550. (b) Naber, R. C. G.; Asadi, K.; Blom, P. W. M.; de Leeuw, D. M.; de Boer, B. *Adv. Mater.* **2009**, *22*, 933–945.
- (2) (a) Takezoe, H.; Kishikawa, K.; Gorecka, E. *J. Mater. Chem.* **2006**, *16*, 2412–2416. (b) Gorecka, E.; Pocięcha, D.; Matraszek, J.; Mieczkowski, J.; Shimbo, Y.; Takaniishi, Y.; Takezoe, H. *Phys. Rev. E* **2006**, *73*, 031704. (c) Gorecka, E.; Pocięcha, D.; Mieczkowski, J.; Matraszek, J.; Guillon, D.; Donnio, B. *J. Am. Chem. Soc.* **2004**, *126*, 15946–15947. (d) Haase, W.; Kilian, D.; Athanassopoulou, M. A.; Knauby, D.; Swager, T. M.; Wrobel, S. *Liq. Cryst.* **2002**, *29*, 133–139. (e) Kishikawa, K.; Nakahara, S.; Nishikawa, Y.; Kohmoto, S.; Yamamoto, M. *J. Am. Chem. Soc.* **2005**, *127*, 2565–2571. (f) Okada, Y.; Matsumoto, S.; Araoka, F.; Goto, M.; Takaniishi, Y.; Ishikawa, K.; Nakahara, S.; Kishikawa, K.; Takezoe, H. *Phys. Rev. E* **2007**, *76*, 041701.
- (3) Fitić, C. F. C.; Tomatsu, I.; Byelov, D.; de Jeu, W. H.; Sijbesma, R. P. *Chem. Mater.* **2008**, *20*, 2394–2404.
- (4) (a) Lightfoot, M. P.; Mair, F. S.; Pritchard, R. G.; Warren, J. E. *Chem. Commun.* **1999**, 1945–1946. (b) Matsunaga, Y.; Miyajima, N.; Nakayasu, Y.; Sakai, S.; Yonenaga, M. *Bull. Chem. Soc. Jpn.* **1988**, *61*, 207–210. (c) Stals, P. J. M.; Smulders, M. M. J.; Martin-Rapun, R.; Palmans, A. R. A.; Meijer, E. W. *Chem.–Eur. J.* **2009**, *15*, 2071–2080.
- (5) (a) Sakamoto, A.; Ogata, D.; Shikata, T.; Urakawa, O.; Hanabusa, K. *Polymer* **2006**, *47*, 956–960. (b) Bushey, M. L.; Nguyen, T. Q.; Nuckolls, C. *J. Am. Chem. Soc.* **2003**, *125*, 8264–8269. (c) Shikata, T.; Kuruma, Y.; Sakamoto, A.; Hanabusa, K. *J. Phys. Chem. B* **2008**, *112*, 16393–16402. (d) Sugita, A.; Suzuki, K.; Kubono, A.; Tasaka, S. *Jpn. J. Appl. Phys.* **2008**, *47*, 1355–1358. (e) Sugita, A.; Suzuki, K.; Tasaka, S. *Chem. Phys. Lett.* **2004**, *396*, 131–135. (f) Sugita, A.; Suzuki, K.; Tasaka, S. *Jpn. J. Appl. Phys.* **2008**, *47*, 8043–8048.
- (6) Rochefort, A.; Bayard, E.; Hadj-Messaoud, S. *Adv. Mater.* **2007**, *19*, 1992–1995.
- (7) (a) Kalinin, S. V.; Bonnell, D. A. *Nano Lett.* **2004**, *4*, 555–560. (b) Kim, Y.; Bae, C.; Ryu, K.; Ko, H.; Kim, Y. K.; Hong, S.; Shin, H. *Appl. Phys. Lett.* **2009**, *94*, 032907.

JA101734G